Design of a radio link network with dc photovoltaic powering for connectivity and smart agriculture in rural areas of Colombia

Diseño de una red de radioenlaces con alimentación fotovoltaica en dc para conectividad y agricultura inteligente en zonas rurales de Colombia

Projeto de uma rede de enlace de rádio alimentada por corrente contínua fotovoltaica para conectividade e agricultura inteligente em áreas rurais da Colômbia

Giovanni Mancilla-Gaona[1]
Carlos Andrés Martínez-Alayón[2]
Gabriel Herrera-Latorre[3]
Michael Andrés Olivares-Herrera[4]

Received: December 9th, 2025
Accepted: March 8th, 2026
Available: May 5th, 2026

How to cite this article:
G. Mancilla-Gaona, C. A. Martínez-Alayón, G. Herrera-Latorre, and M. A. Olivares-Herrera, "Design of a Radio Link Network with DC Photovoltaic Powering for Connectivity and Smart Agriculture in Rural Areas of Colombia," *Revista Ingeniería Solidaria*, vol. 22, no. 2, 2026.
doi: https://doi.org/10.16925/2357-6014.2026.02.02

Research article. https://doi.org/10.16925/2357-6014.2026.02.02

[1] Faculty of Engineering, Universidad Distrital Francisco José de Caldas, Bogotá, Colombia.
Email: gmancillag@udistrital.edu.co
ORCID: https://orcid.org/0000-0002-2552-1836
CvLAC: https://scienti.minciencias.gov.co/cvlac/visualizador/generarCurriculoCv.do?cod_rh=0001335300

[2] Faculty of Engineering, Universidad Distrital Francisco José de Caldas, Bogotá, Colombia.
Email: camartineza@udistrital.edu.co
ORCID: https://orcid.org/0000-0003-0818-7095
CvLAC: https://scienti.minciencias.gov.co/cvlac/visualizador/generarCurriculoCv.do?cod_rh=0001366648

[3] Faculty of Engineering, Universidad Distrital Francisco José de Caldas, Bogotá, Colombia.
Email: gherreral@udistrital.edu.co
ORCID: https://orcid.org/0009-0005-7093-5690
CvLAC: https://scienti.minciencias.gov.co/cvlac/visualizador/generarCurriculoCv.do?cod_rh=0002369488

[4] Faculty of Engineering, Universidad Distrital Francisco José de Caldas, Bogotá, Colombia.
Email: maolivaresh@udistrital.edu.co
ORCID: https://orcid.org/0009-0009-2915-1762
CvLAC: https://scienti.minciencias.gov.co/cvlac/visualizador/generarCurriculoCv.do?cod_rh=0002372223

Abstract

Introduction: This article is a product of the research project “Design of a Radio Link Network with DC Photovoltaic Powering for Connectivity and Smart Agriculture in Rural Areas of Colombia”, developed at the Universidad Distrital Francisco José de Caldas in 2025.

Problem: The digital divide in Colombia’s rural areas restricts educational and productive development due to high costs and the lack of coverage from traditional telecommunications services.

Objective: To design a radio link network with direct current (DC) photovoltaic power to enable connectivity and smart agriculture in the study area.

Methodology: The preparation, planning, and design phases of the Cisco PPDIOO methodology were applied. Topographic analysis and simulations were performed using Xirio Online software to validate links in the 5.8 GHz band.

Results: The simulations confirmed technical feasibility, with fade margins exceeding 20 dB and optimal reception levels (-63 dBm). The energy system ensures 18 hours of autonomy, powering the equipment directly.

Conclusion: The proposed design constitutes a robust, scalable, and energy-efficient solution, technically viable for bridging the digital divide and fostering agricultural modernization in communities without a conventional power grid.

Originality: The project introduces an innovative direct current (DC) photovoltaic power system that eliminates the use of inverters to maximize efficiency and guarantee the autonomy of the repeater node.

Limitations: Operation in the unlicensed spectrum carries interference risks; therefore, implementation requires on-site spectrum analysis to validate that the noise floor does not degrade the calculated margin.

Keywords: Radio links; agriculture; rural areas; solar energy; telecommunications; digital divide.

Resumen

Introducción: Este artículo es producto de la investigación “Diseño de una Red de Radioenlaces con Alimentación Fotovoltaica en DC para Conectividad y Agricultura Inteligente en Zonas Rurales de Colombia”, desarrollada en la Universidad Distrital Francisco José de Caldas en el año 2025.

Problema: La brecha digital en las zonas rurales de Colombia restringe el desarrollo educativo y productivo debido a los altos costos y la falta de cobertura de los servicios tradicionales de telecomunicaciones.

Objetivo: Diseñar una red de radioenlaces con alimentación fotovoltaica en corriente continua (DC) para habilitar la conectividad y la agricultura inteligente en el área de estudio.

Metodología: Se aplicaron las fases de preparación, planeación y diseño de la metodología Cisco PPDIOO. Se realizaron análisis topográficos y simulaciones con el software Xirio Online para validar los enlaces en la banda de 5.8 GHz.

Resultados: Las simulaciones confirmaron la viabilidad técnica, con márgenes de desvanecimiento superiores a 20 dB y niveles de recepción óptimos (-63 dBm). El sistema energético asegura 18 horas de autonomía, alimentando los equipos directamente.

Conclusión: El diseño propuesto constituye una solución robusta, escalable y energéticamente eficiente, técnicamente viable para cerrar la brecha digital y fomentar la modernización agrícola en comunidades sin red eléctrica convencional.

Originalidad: El proyecto introduce un sistema de potencia fotovoltaico en corriente continua (DC) innovador que elimina el uso de inversores para maximizar la eficiencia y garantizar la autonomía del nodo repetidor.

Palabras clave: Radioenlaces; agricultura; zonas rurales; energía solar; telecomunicaciones; brecha digital.

Resumo

Introdução: Este artigo é produto do projeto de pesquisa "Projeto de uma Rede de Rádio CC Alimentada por Energia Fotovoltaica para Conectividade e Agricultura Inteligente em Áreas Rurais da Colômbia", realizado na Universidade Distrital Francisco José de Caldas em 2025.

Problema: A exclusão digital em áreas rurais da Colômbia restringe o desenvolvimento educacional e produtivo devido aos altos custos e à falta de cobertura dos serviços tradicionais de telecomunicações.

Objetivo: Projetar uma rede de rádio CC alimentada por energia fotovoltaica para viabilizar conectividade e agricultura inteligente na área de estudo.

Metodologia: As fases de preparação, planejamento e projeto da metodologia Cisco PPDIOO foram aplicadas. Análises topográficas e simulações foram realizadas utilizando o software Xirio Online para validar os enlaces na banda de 5,8 GHz.

Resultados: As simulações confirmaram a viabilidade técnica, com margens de desvanecimento superiores a 20 dB e níveis de recepção ótimos (-63 dBm). O sistema de energia garante 18 horas de autonomia, alimentando diretamente os equipamentos.

Conclusão: O projeto proposto constitui uma solução robusta, escalável e energeticamente eficiente, tecnicamente viável para reduzir a exclusão digital e promover a modernização agrícola em comunidades sem uma rede elétrica convencional.

Originalidade: O projeto introduz um sistema inovador de energia fotovoltaica de corrente contínua (CC) que elimina o uso de inversores para maximizar a eficiência e garantir a autonomia do nó repetidor.

Palavras-chave: Enlaces de rádio; agricultura; áreas rurais; energia solar; telecomunicações; exclusão digital.

INTRODUCTION

Information and Communication Technologies (ICT) have become fundamental pillars of economic development and social equity; however, a significant digital divide persists, marginalizing rural communities. In the Colombian context, this inequality is reflected in the indicators of the ENTIC Households survey, which identifies the main barriers to Internet access in these areas as high service costs (48.6%) and limited technical coverage (11.1%) [1]. These limitations restrict access to quality educational opportunities and hinder the modernization of agricultural production processes, perpetuating cycles of technological lag.

Furthermore, the global transition toward Agriculture 4.0 requires a robust connectivity infrastructure that enables the integration of Internet of Things (IoT) sensors and data analytics in the field. In rural Colombia, the absence of this digital ecosystem prevents small-scale producers from optimizing water resources and improving crop yields through precision monitoring.

This situation is particularly evident in the Buenos Aires district, municipality of La Calera (Cundinamarca), where complex orographic conditions, characterized by mountainous terrain and geographic dispersion, hinder connectivity. For the student population, this limitation restricts access to digital educational resources, while for farmers, it represents a barrier to implementing smart agriculture techniques, consulting weather forecasts, and accessing real-time market prices. Additionally, preliminary terrain analysis revealed a lack of direct Line of Sight (LoS) between the points of interest, making the strategic placement of repeater nodes necessary to overcome natural obstacles.

Given this scenario, it is essential to consider alternatives that are both technically and economically viable. Comparative studies indicate that the deployment of fiber optics in rugged terrain can exceed 350 million COP, making its immediate implementation unfeasible [2]. Meanwhile, satellite solutions, although offering global coverage, involve recurring operating expenses (OPEX) that are unsustainable for social projects [3]. In contrast, radio links emerge as the most appropriate strategic option, given their low implementation cost (CAPEX) and the absence of monthly spectrum fees in unlicensed bands [4].

The purpose of this article is to present the technical design of a high-availability radio link network, conceived as a replicable solution for complex rural environments. The development is based on the Cisco PPDIOO life cycle (Prepare, Plan, Design, Implement, Operate, and Optimize) [5], a framework that ensures the scalability and resilience of the network architecture.

Moreover, the project introduces an innovative direct current (DC) photovoltaic power system. This energy architecture eliminates efficiency losses associated with DC–AC–DC conversion by removing inverters, thereby maximizing energy harvesting and ensuring the autonomy of the repeater node in areas without access to the electrical grid. This approach demonstrates the feasibility of a sustainable model that integrates high-speed connectivity with renewable energy solutions.

1. MATERIALS AND METHODS

The technical rigor of this engineering design is based on the integration of high-precision simulation tools and hardware components optimized for critical rural environments. The methodological approach seeks not only to ensure the technical feasibility of the wireless link but also to guarantee the energy sustainability of the system through an architecture that minimizes conversion losses. To achieve this, industrial-grade materials and specialized telecommunications equipment were selected to withstand the demanding orographic conditions of the Buenos Aires district and the absence of conventional electrical infrastructure. This selection ensures that the design remains scalable and replicable in other regions with similar characteristics.

Furthermore, the methodology incorporates advanced terrain profiling and radio-frequency (RF) propagation modeling to predict signal behavior under adverse weather conditions. By combining empirical site data with computational analysis, the design bridges the gap between theoretical link budgets and real-world deployment performance, establishing a robust framework for rural connectivity projects.

1.1. Simulation and Modeling Tools

For the design phase and theoretical validation of the radio link, specialized software tools were employed to model electromagnetic propagation behavior:

Xirio Online: This professional radio planning platform [6] was used to perform detailed calculations of elevation profiles and to determine Fresnel zones. This tool enabled the application of advanced propagation models to validate technical feasibility in the 5.8 GHz band, taking into account the orographic obstructions identified in the study area [7]. The use of this platform ensured a high degree of correlation between simulated results and potential field performance by accounting for diffraction losses and atmospheric attenuation.

Google Earth Pro: This tool served as the primary cartographic support for the precise positioning of node geographic coordinates using the WGS84 coordinate system [8]. Its 3D visualization capabilities facilitated a preliminary inspection of the Line of Sight (LoS) and the validation of Euclidean distances between transmission and reception points. This spatial analysis was essential for identifying strategic locations for repeater nodes to overcome terrain-related signal obstruction.

Photovoltaic Modeling: The estimation of energy production was based on historical solar irradiance databases for the Cundinamarca region [9]. This multi-year data analysis ensures that the solar system design can meet the continuous energy demand of the telecommunications equipment throughout the year, even during periods of low solar radiation (worst-case scenario planning).

1.2. Implementation of the DC Photovoltaic System

The design proposes a high-efficiency energy infrastructure based exclusively on direct current (DC) to power the communication nodes:

Bifacial Solar Panels: High-efficiency bifacial photovoltaic modules were selected to maximize energy harvesting by capturing solar radiation from both the front and rear surfaces [10]. This technology is particularly effective in rural mountainous areas, where albedo effects from the surrounding terrain can significantly increase total power generation.

MPPT Charge Controllers: Energy management is handled by charge controllers using Maximum Power Point Tracking (MPPT) algorithms [11]. These devices optimize impedance matching between the PV array and the storage system, ensuring maximum power transfer under varying environmental conditions such as temperature and irradiance fluctuations.

Deep-Cycle Batteries: The storage subsystem consists of deep-cycle batteries sized to provide 18 hours of autonomy [12]. The use of deep-cycle technology ensures the system can withstand repeated discharge cycles without significant degradation, maintaining network availability during nighttime and consecutive cloudy days.

DC-DC Boost Converters: To achieve the specific operating voltage levels required by the telecommunications equipment, high-efficiency DC-DC boost converters were integrated [13]. By maintaining the entire system in DC, the design eliminates the need for conventional AC inverters, thereby avoiding efficiency losses associated with DC–AC–DC double conversion and reducing overall system complexity and potential points of failure.

Electrical Protection System: To safeguard the integrity of the active equipment, the design incorporates a robust protection stage. This includes surge protection devices (SPD), DC breakers, and grounding systems specifically designed for rural environments. These components are essential to mitigate risks associated with atmospheric discharges and transient overvoltages, ensuring the long-term reliability of the repeater node.

1.3 Telecommunications and Powering Equipment

The selection of active and passive components was driven by the need for high energy efficiency and resilience in remote environments:

Radwin IDU Unit: The design integrates a Radwin series Indoor Unit (IDU) [14], specifically selected for its native compatibility with DC voltage input. This component serves as the cornerstone of the proposed direct current electrical architecture, enabling seamless integration with the photovoltaic system without the need for intermediate inversion stages. This direct coupling significantly reduces the thermal footprint and potential failure points within the repeater station.

DC-PoE Injectors and Chargers: To interface the power system with the outdoor radio units (ODU), specialized passive PoE (Power over Ethernet) injectors were incorporated. These devices function as DC-DC chargers that regulate the voltage from the battery bank to the specific levels required by the antennas (typically 24 V or 48 V DC), enabling the transmission of both high-speed data and electrical power over a single Ethernet cable. This configuration simplifies cabling and minimizes voltage drops over long vertical runs on towers.

Support Infrastructure: The design includes communication towers and specialized mounting hardware to ensure signal integrity and the physical stability of the equipment at strategic locations within the Buenos Aires district. Mechanical stability is prioritized to maintain precise antenna alignment, which is critical for sustaining high-capacity links in areas exposed to high wind speeds and adverse weather conditions.

1.4. Methodological Procedure

The technical deployment of the network proposed in this research was rigorously based on the first three phases—Prepare, Plan, and Design—of the Cisco Systems PPDIOO lifecycle. This methodology is widely recognized in the specialized literature as a standard and robust framework for the deployment of telecommunications infrastructure [5]. As illustrated in Figure 1, this cyclic model enables comprehensive network management, ensuring that each engineering stage responds to a prior analysis of needs and feasibility.

The selection of this methodological framework is justified by its proven effectiveness in executing connectivity projects across various complex scenarios, with particular emphasis on bridging the digital divide in rural areas. By adopting this approach, the present study ensures a logical transition from the identification of social requirements to technical validation through simulation, allowing the design to be scalable for other communities with similar geographic challenges.

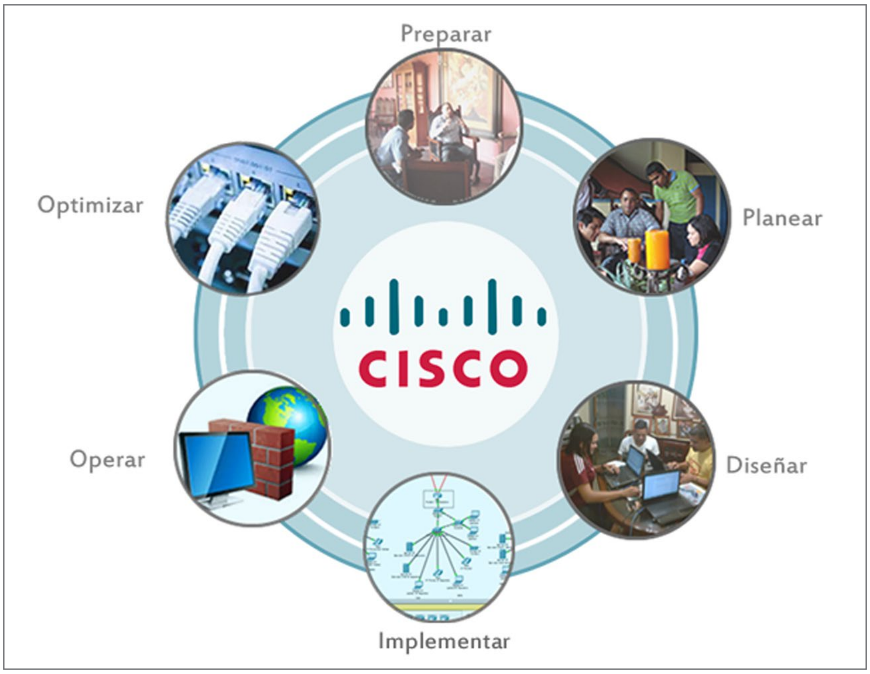

Figure 1. Phases of the Cisco PPDIOO Methodology
Note. The diagram illustrates the lifecycle for network design and management.
Adapted from CCDA 200-310 Official Cert Guide (5th ed.) [5].

1.4.1. Preparation Phase

In the initial phase, the strategic and technical foundations were defined based on the core problem: the lack of connectivity at the rural school in the Buenos Aires district (see Figure 2). This situation reflects the digital divide affecting rural areas in Colombia, where it is estimated that 48.6% of households do not have Internet access due to high costs, and 11.1% lack access due to insufficient coverage [1].

Figure 2. Aerial view of the rural school in Buenos Aires.

To address this problem, the feasibility of establishing a radio link between the "Radio Teusacá" Institutional Radio Station and the educational institution was analyzed (see Figure 3). However, the preliminary topographic study showed that the mountainous terrain prevents a direct line of sight between the points. As observed in the elevation profile in Figure 4, the presence of orographic obstructions required the inclusion of an intermediate relay node in the final design to ensure signal propagation.

Figure 3. Distance between the "Radio Teusacá" Institutional Radio Station and the rural school.

Following the identification of the geographic distance between the two points, a detailed analysis of the terrain's vertical geometry was necessary. This evaluation allowed for the detection of critical landforms that could potentially interrupt the signal's path before finalizing the network topology.

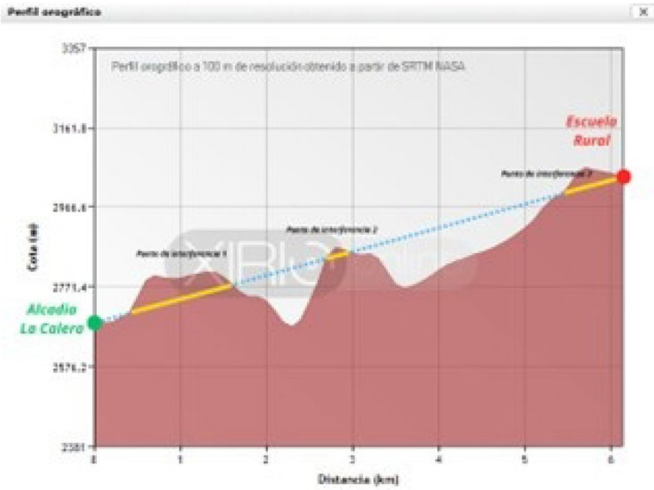

Figure 4. Elevation Profile with Obstruction Points.
Note. Generated elevation profile showing topographic obstruction points in the direct path between the La Calera Mayor's Office and the rural school.

Finally, regulatory compliance was verified according to Resolution 105 of 2020 of the National Spectrum Agency (ANE) [15]. This regulation allows for the free use of the 5.8 GHz band, which eliminates licensing costs, provided that the Equivalent Isotropically Radiated Power (EIRP) does not exceed 36 dBm [15]. Although this regime facilitates deployment, it carries a risk of interference due to the lack of spectrum protections, a factor that was analyzed in subsequent design phases. The technical parameters are summarized in Table 1.

Table 1. Operating Parameters in the 5.8 GHz Band according to the ANE.

Application Frequency	Application Name	Technical and Operational Conditions	Associated Regulations
5725 MHz 5875 MHz	Non-specific short-range radiocommunication applications	Maximum electric field strength of 50 mV/m measured at 3 m	ANE Resolution 105 of 03/27/2020

Note. The data corresponds to Annex 1 on Unlicensed Frequencies. Adapted from the National Spectrum Agency [15].

1.5 Planning Phase

A. Definition of Requirements and Bandwidth Estimation

Through technical field inspections and structured interviews with teaching staff, it was determined that the network will serve a community of 42 fixed users (40 students and two teachers) and 17 additional members from the district. The infrastructure includes 15 computers for student use, which establishes the baseline for simultaneous connection density. Based on this census, functional requirements were defined, prioritizing access to audiovisual resources [17], interactive learning tools [18], national educational platforms [19], and continuous teacher training spaces [20].

The bandwidth calculation was based on industry standards, taking as a reference the recommendations for high-definition video transmission (HD 720p), which requires a rate of 2.5 Mbps to guarantee an adequate Quality of Experience (QoE) [21]. These parameters are detailed in Table 2.

Table 2. Recommended Connection Speeds for YouTube.

Video Resolution	Recommended Sustained Speed
4K UHD	20 Mbps
HD 1080p	5 Mbps
HD 720p	2.5 Mbps
SD 480p	1.1 Mbps

Note. Data obtained from the YouTube System Requirements Guide [21].

Additionally, for general web browsing, a conservative standard of 1 Mbps per concurrent user was applied, following the guidelines of the Federal Communications Commission (FCC) [22], which are summarized in Table 3.

Table 3. Minimum Download Speed by Activity according to the FCC.

Activity	Minimum Download Speed (Mbps)
General Use	
General browsing and email	1
Social media	1
Calls	Less than 0.5
Video	
Standard Definition (SD) video streaming	3 – 4
High Definition (HD) video streaming	5 – 8
Video Conferencing	
Standard personal video call	1
HD personal video call	1.5

Note. Data adapted from the FCC Broadband Speed Guide [22].

Based on these analyses, a maximum simultaneous demand scenario was modeled, considering one HD video session and 15 users actively browsing the web. The results of this size are presented in Table 4.

Table 4. Minimum Bandwidth Calculation in a Maximum Demand Scenario.

Traffic Type	Required Bandwidth	Technical Justification
Video Streaming (HD 720p)	2.5 Mbps	Based on the YouTube standard for 720p video [9].
Web Browsing (15 users)	15.0 Mbps	1 Mbps per user, based on FCC guidelines [10].
Operating Margin	5.25 Mbps	To absorb peaks, background traffic, and protocol overhead.
Total Required (Download)	~23 Mbps	Sum of requirements and safety margin.
Total Required (Upload)	5 Mbps	To support occasional video calls and file uploads.

Note. Author’s own elaboration.

It was concluded that the design must stably guarantee a performance of 23 Mbps download and 5 Mbps upload to satisfy the needs of the educational community.

B. Selection of Radio Link Equipment

To meet the technical and energy efficiency requirements, equipment from the Radwin 5000 series was selected. The architecture consists of a High-capacity Subscriber Unit (HSU) at the radio station (source), a High-capacity Base Station (HBS) operating as a relay point on the hill, and another HSU at the school (destination). This configuration leverages a Point-to-MultiPoint (PtMP) topology, which optimizes spectral efficiency and allows for future network expansion to other points within the district without requiring a complete infrastructure overhaul. The technical comparison justifying this choice is presented in Table 5.

Table 5. Technical Comparison of Available Radio Link Equipment.

Feature	Radwin 5000 JET	Radwin HSU 550
Model	RW-5BG5-9650	RW-5550-9H54
Type	Base Station (PtMP)	Subscriber Unit (PtMP)
Maximum Capacity	750 Mbps	50 Mbps
Antenna Gain	20 dBi	23 dBi
Beamwidth	90° (Sectoral)	10° (Directive)
Max. Tx Power	25 dBm	21 dBm
Power Consumption	< 30 W	< 12 W

Note. Data extracted from technical specification sheets provided by the manufacturers [23], [24].

The selection of Radwin technology is further supported by its robust Air Interface protocol, which provides mitigation against the interference risks inherent in the unlicensed 5.8 GHz band. Additionally, its low power consumption profiles are critical for maintaining the 18-hour autonomy target defined in the energy subsystem design.

1.5.1 Design Phase

This stage transforms the requirements into a definitive technical solution, encompassing the network architecture, the power system, and the radio link engineering. A three-node topology was developed to bypass topographic interruptions:

Source Node: Located on the "Radio Teusacá" Institutional Radio Station tower within the urban area of La Calera, leveraging existing infrastructure and internet access.
Relay Node (Repeater): Situated on "Cerro de la Pita," a high-altitude geographical point that guarantees Line of Sight (LoS) with the other two nodes. This strategic placement acts as a bridge to overcome the signal masking caused by the mountainous terrain, ensuring the continuity of the first Fresnel zone across the link.
Destination Node: Installed at the Buenos Aires Rural School to provide the final connectivity coverage.

Figure 5. Network architecture and node location.
Note. Author's own elaboration based on Google Earth data [8].

A. Photovoltaic Power System Design

The main challenge at the relay node was the lack of an electrical grid; therefore, a direct current (DC) photovoltaic system was implemented to ensure continuous operation and maximize energy efficiency. Although the node consumes 35 W, the system was sized for 80 W, thus guaranteeing scalability and the potential addition of new equipment without the need to redesign the power source.

Design Parameters

The main parameters established for the sizing were as follows:

Node design power: 80 W.
Operating time: 24 h/day.
Required autonomy: 18 h.
Maximum Depth of Discharge (DoD): 40%.
Battery bank voltage: 24 V.
Assumed overall system efficiency (MPPT, cabling, etc.): η = 0.85.
Average Peak Sun Hours (PSH) in La Calera: 5 h.
Selected Panel: 625 Wp Vmp = 41.7 V, Imp = 15.0 A, Voc = 49.9 V, Isc 16.7 A.

Daily Consumption Calculation

The total energy consumption of the node was determined using the following equation:

$$E_{day} = P_{node} \cdot t_{operation}$$

$$E_{day} = P \times t = 80\,W \times 24\,h = 1920\,Wh/day$$

Sizing of the Battery Bank

To guarantee an autonomy of 18 hours in the absence of solar radiation, the required energy was calculated as:

$$E_{required} = P_{node} \cdot t_{autonomy}$$

$$\mathrm{E}_{required} = 80\ \mathrm{W} \times 18\ \mathrm{h} = 1440\ \mathrm{Wh}$$

Considering a maximum Depth of Discharge (DoD) of 40%, the total capacity of the bank resulted in:

$$C_{\text{total(Wh)}} = \frac{E_{required}}{\text{DoD}} = \frac{1440}{0.4} = 3600 \text{ Wh}$$

For a 24 V system, the equivalent capacity was:

$$C_{\text{Ah}} = \frac{3600 \text{ Wh}}{24 \text{ V}} = 150 \text{ Ah}$$

Consequently, a 150 Ah at 24 V battery bank was selected, configured using two 12 V, 150 Ah batteries connected in series.

Photovoltaic System Power Calculation

The energy to be generated by the panels to supply daily consumption and compensate for system losses was estimated as:

$$E_{\text{gen}} = \frac{E_{\text{day}}}{\eta} = \frac{1920 \text{ Wh/day}}{0.85} \approx 2258.82 \text{ Wh/day}$$

With an average of 5 peak sun hours (PSH), the minimum peak power required was:

$$P_{\text{peak}} = \frac{E_{gen}}{\text{HSP}} = \frac{2258.82 \text{ Wh}}{5 \text{ h}} \approx 451.76 \text{ Wp}$$

Since 625 Wp panels were selected, a single panel was sufficient to cover the daily demand with a safety margin. The panel produces approximately:

$$E_{\text{panel}} = 625 \text{ W} \times 5 \text{ h} \times 0.85 = 2656.25 \text{ Wh/día}$$

Therefore, the energy generated by one panel exceeds the system's requirements.

Charge Controller Sizing (MPPT)

The selected panel features the following electrical parameters:

$$\mathrm{Vmp} = 41.7\ \mathrm{V},\ \mathrm{Imp} = 15.0\ \mathrm{A},\ \mathrm{Voc} = 49.9\ \mathrm{V},\ \mathrm{Isc} = 16.7\ \mathrm{A}.$$

The theoretical charging current toward the 24 V bank was estimated at:

$$\mathrm{I}_{\mathrm{charge\_theory}} = \frac{625\ \mathrm{W}}{24\ \mathrm{V}} \approx 26.0\ \mathrm{A}$$

Considering the system efficiency, the actual charging current was:

$$\mathrm{I}_{chargeReal} \approx \mathrm{I}_{chargeTheory} \cdot \ \eta$$

$$\mathrm{I}_{chargeReal} \approx 26.0\ \mathrm{A} \times 0.85 = 22.1\ \mathrm{A}$$

Consequently, a 30 A MPPT controller was chosen, with sufficient capacity to withstand the panel's short-circuit current (Isc * 1.25 = 20.9A) and allow for future expansions.

Recharge Time Estimation

The effective power supplied by the panel to the system was:

$$\mathrm{P}_{\mathrm{eff}} = \mathrm{P}_{\mathrm{Wp}} \cdot \eta \ = \ 625\mathrm{W} \times 0.85 = 531.25\ \mathrm{W}$$

The time required to replenish the daily consumption was determined as:

$$\mathrm{t}_{\mathrm{recharge}} = \frac{\mathrm{E}_{\mathrm{day}}}{\mathrm{P}_{\mathrm{eff}}} = \frac{1920\ \mathrm{Wh}}{531.25\ \mathrm{W}} \approx 3.6\ \mathrm{h}$$

This value indicates that, under average irradiance conditions, the total daily energy consumed can be fully recovered in less than four effective hours.

DC/DC Boost Converter for Equipment Powering

The Radwin equipment operates at 48 V, while the battery bank delivers 24 V. For this reason, a DC/DC boost converter with an approximate efficiency of 95% was implemented, capable of transforming the 24 V from the bank into a 48 V output. The current demanded by the equipment at 48 V was:

$$\mathrm{I}_{48\mathrm{V}} = \frac{P_{node}}{V_{out}} = \frac{80\ \mathrm{W}}{48\ \mathrm{V}} \approx 1.67\ \mathrm{A}$$

And the current drawn from the 24 V bank was:

$$\mathrm{I}_{24} = \frac{P_{node}}{V_{in} \cdot \eta_{\mathrm{conv}}} \frac{80\ \mathrm{W}}{24\ \mathrm{V} \times 0.95} \approx 3.51\ \mathrm{A}$$

Therefore, a 100 W nominal converter with a 48 V / 3 A output was selected, guaranteeing continuous operation without overload.

Additional Considerations and Protections

During the design, the following protection measures were incorporated:

PV Fuse: 25 A on the panel line, equivalent to 1.25 * Isc.

Circuit Breaker: 30–40 A between the regulator and the battery bank.

Output Protection: 10 A at the DC/DC converter output.

General Protections: Reverse polarity protection, disconnectors for maintenance, and thermal protection for both the MPPT and the converter.

The system operates with a C-rate of 0.15C, an appropriate value to guarantee a long service life for the battery bank.

B. Radio Link Network Design

To guarantee a robust and reliable connection that met the bandwidth requirements, the radio link network design focused on two fundamental aspects: signal path analysis and the power budget calculation to ensure an adequate operating margin.

Line of Sight and Fresnel Zone Analysis

Every microwave radio link requires a clear Line of Sight (LoS). The signal does not travel in a perfectly straight line, but rather within an ellipsoidal volume known as the Fresnel Zone, where partial obstruction causes diffraction losses. Therefore, it is recommended to maintain at least 60% clearance of the first zone's radius [16]. The maximum radius is determined according to the following equation:

$$r_1 = 17.32 \cdot \sqrt{\frac{d_{km}}{4 \cdot f_{GHz}}}$$

Link Power Budget

The power balance accounts for the gains and losses of the system, allowing for the determination of the Received Signal Level (RSL) and the Fade Margin, which are two of the link's primary quality indicators. The fundamental equation is as follows:

$$RSL_{(dBm)} = P_{TX(dBm)} + G_{TX(dBi)} - L_{Total(dB)} + G_{RX(dBi)}$$

Equivalent Isotropically Radiated Power (EIRP)

EIRP represents the total power that a theoretical isotropic antenna would emit to produce the same signal intensity as the actual antenna in its direction of maximum gain. It is calculated as:

$$EIRP_{dBm} = P_{TX(dBm)} + G_{TX(dBi)}$$

Total Path Losses

This term groups all the attenuations experienced by the signal:

$$L_{Total(dB)} = L_{fs(dB)} + L_{gases(dB)} + L_{rain(dB)} + L_{misc(dB)}$$

Fade Margin (FM)

It is the most important reliability metric. It represents the amount of additional attenuation (primarily due to rain) that the link can withstand before falling below the receiver's minimum sensitivity (R_s):

$$FM_{(dB)} = RSL_{(dBm)} - R_{s(dBm)}$$

For this project, a sensitivity (R_s) of $-85\mathrm{dBm}$ is assumed, which is the threshold necessary to maintain stable and high-capacity modulation.

Quantitative Evaluation of the Theoretical Radio Link (Section A)

In order to validate the design and establish a quantitative basis, the complete link budget calculation for Section A (Radio Station - Hill) is presented. This exercise provides the answer to what the theoretical performance of the system would be assuming optimal propagation conditions (without obstruction of the Fresnel zone); in such a way that the results obtained will serve as a reference value to compare against the data obtained in the simulation, thus allowing for the unraveling of the real effect produced by the terrain topography.

$$P_{TX(HSU)} = 11\ dBm \qquad P_{TX(HBS)} = 20\ dBm$$

$$G_{TX(HSU)} = 23\ dBi \qquad G_{RX(HBs)} = 20\ dBi$$

$$d_1 =: 2.8\ km \qquad d_2 = 2.8\ km$$

$$f =: 5800\ MHz$$

For the direct path (Radio Station - Hill), the effective isotropically radiated power (EIRP) was first calculated. This is equal to the optimized power emitted by the HSU (11 dBm) plus the gain of said antenna (23 dBi).

$$EIRP = 11dBm + 23\ dBi = 34\ dBm$$

Next, the fixed path losses are calculated. The free space path loss (L_{fs}) for 2.8 km at 5800 MHz is the primary component.

$$L_{fs} = 32.45 + 20\log_{10}(2.8\ km) + 20\log_{10}(5800) = 116.66\ dB$$

The total attenuation (L_{Total}) is obtained by adding the free space path loss, the attenuation due to gases (0.056 dB), and miscellaneous losses (1.5 dB).

$$L_{Total} = 116.66\ dB + 0.056\ dB + 1.5\ dB = 118.22\ dB$$

With these values, we can calculate the theoretical Received Signal Level (RSL), having already considered the gain of the receiving HBS antenna (which is equal to 20 dBi).

$$RSL = 34\ dBm - 118.22 dB + 20 dBi = -64.22\ dBm$$

Finally, we will determine the theoretical Fade Margin (FM), which is the power reserve in the link relative to the receiver sensitivity (which is equal to -85 dBm).

$$FM = -64.22\ dBm - (-85\ dBm) = 20.78\ dB$$

Quantitative Evaluation of the Theoretical Link (Section B)

For the second section, the transmitter is the HBS located at the Hill. Its EIRP is calculated by adding its optimized power (20 dBm) and its antenna gain (20 dBi).

$$EIRP = 20\ dBm + 20\ dBi = 40\ dBm$$

The free space path losses for the 8.1 km distance are considerably higher.

$$L_{fs} = 32.45 + 20\log_{10}(8.1\ km) + 20\log_{10}(5800) = 125.87\ dB$$

By adding the gas losses (0.162 dB) and miscellaneous losses (1.5 dB), the total attenuation for this section is 127.53 dB.

$$L_{Total} = 125.87\ dB + 0.162\ dB + 1.5\ dB = 127.53\ dB$$

The RSL at the School is then projected, considering the gain of the receiving HSU antenna (23 dBi).

$$RSL = 40\ dBm - 127.53\ dB + 23\ dBi = -64.53\ dBm$$

The theoretical Fade Margin for the longest section is determined below.

$$FM = -64.53\ dBm - (-85\ dBm) = 20.47\ dB$$

The results obtained in the theoretical analysis reflect a robust and balanced performance for both segments of the network. It is observed that, although Section B has a length nearly three times greater than Section A, the strategic use of higher transmission power at the Base Station (HBS) and the high gain of the receiving antenna (HSU) effectively compensate for the increase in free space path losses (see Figure 5 and Table 6). Under these conditions, both links are projected to operate with received signal levels (RSL) close to the target of -65 dBm and fade margins exceeding 20 dB. These indicators guarantee, from a theoretical perspective, high availability and service stability. However, the subsequent simulation phase is fundamental to contrast these values against a Digital Terrain Model (DTM), allowing for the evaluation of the real impact of topographic conditions and orographic obstructions on signal propagation.

Table 6. Theoretical Parameters Comparison by Link Segment.

Feature	Section A (Station → Hill)	Section B (Hill → School)
Distance	2.8 km	8.1 km
Tx Power	11 dBm	20 dBm
Tx Antenna Gain	23 dBi	20 dBi
EIRP	34 dBm	40 dBm
Total Path Loss	118.22 dB	127.53 dB
Rx Antenna Gain	20 dBi	23 dBi
RSL	-64.22 dBm	-64.53 dBm
Fade Margin (FM)	20.78 dB	20.47 dB

Note. Author's own elaboration.

C. Link-by-Link Simulation for Design Verification

To refine the theoretical design and characterize the performance of the radio links under real-world Digital Terrain Models (DTM), the Xirio Online software platform was utilized [6]. This professional planning tool bases its computational algorithms on Recommendation ITU-R P.530-17, which constitutes the international standard for the planning and prediction of propagation effects in terrestrial fixed wireless systems [7]. This methodological approach ensures that the simulations account for critical phenomena such as multipath fading and atmospheric refraction.

The simulation process was systematically structured into three fundamental stages:

Geospatial Characterization of Sites: In this phase, the precise geographical coordinates and altitudes for the three network nodes—Radio Station, Cerro La Pita, and School—were defined. This step is essential for integrating high-resolution cartographic data, enabling the identification of potential orographic obstacles along the path.

Technical Parameterization of Equipment: The technical profiles for the Radwin HSU 550 and Radwin 5000 JET systems were configured [23][24]. Critical operational parameters were meticulously defined, including optimized transmission power, antenna gain patterns, and receiver sensitivity thresholds. This ensures that the digital representation of the hardware accurately reflects its real-world performance.

Link Synthesis and Study Configuration: Finally, specific radio link studies were established for Section A and Section B. By associating the defined sites and equipment, the software executed complex calculations to determine quality and availability indicators. This stage enables the transition from a theoretical free-space model to a deterministic model influenced by the specific topography of the region.

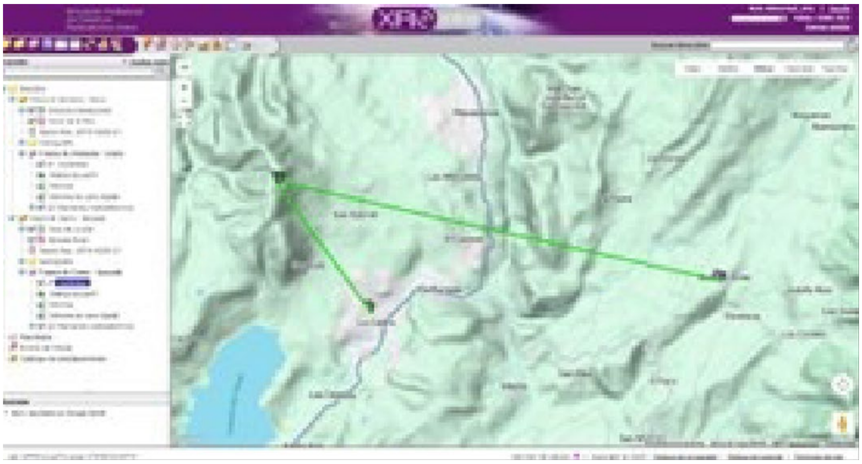

Figure 6. Simulation parameter configuration.
Note. Author's own elaboration based on the Xirio Online interface [6].

2. RESULTS

This section objectively presents the final, quantifiable outputs of the design process, derived from high-fidelity simulations performed using the Xirio Online platform [6]. These results constitute the technical validation of the proposed network architecture and serve as the baseline for subsequent performance analysis. The final network architecture is illustrated in Figure 7, which depicts the strategic positioning of the three nodes and the two interconnecting radio links. This layout is overlaid on a high-resolution Digital Terrain Model (DTM) of the study area, allowing for a precise visualization of the geospatial relationship between the urban source and the rural destination. The selection of these sites was determined by the requirement for a clear Line of Sight (LoS) and the minimization of orographic obstructions within the first Fresnel zone.

Figure 7. Network architecture and node location.
Note. Author's own elaboration based on data from Xirio Online [6] and Google Earth [8].

To ensure system reliability, the technical profiles of the selected radio equipment were meticulously parameterized. Table 7 summarizes the hardware specifications for each node, emphasizing their technical functions and optimized transmission power levels. These power settings were specifically calibrated to balance energy efficiency—a critical factor for the solar-powered relay node—with the need to maintain robust link margins under environmental attenuation conditions.

e-ISSN 2357-6014 / Vol. 22, no. 2 / may-august 2026 / Bogotá D.C., Colombia
Universidad Cooperativa de Colombia

Table 7. Selected Equipment and Node Configuration.

Node	Assigned Equipment	Model	Function	Tx Power
Institutional Radio Station	RADWIN HSU 550	RW-5550-9H54	Access Point (AP) – Source	11 dBm
Cerro La Pita	RADWIN 5000 JET	RW-5BG5-9650	Base Station (PtMP) – Repeater	20 dBm
Rural School	RADWIN HSU 550	RW-5550-9H54	Subscriber (CPE) – Destination	11 dBm

Note. Power configurations correspond to optimized values determined for this specific design [23][24].

2.1. Simulation Results for Section A (Radio Station → Hill)

The initial link, spanning a distance of 2.88 km, underwent rigorous computational analysis to evaluate its orographic viability and radioelectric performance. Figure 8 illustrates the terrain path profile, which serves as a primary diagnostic tool to confirm a clear Line of Sight (LoS). The visualization verifies that the first Fresnel zone remains unobstructed by topographical features or artificial structures, a critical requirement for minimizing diffraction losses in the 5.8 GHz band.

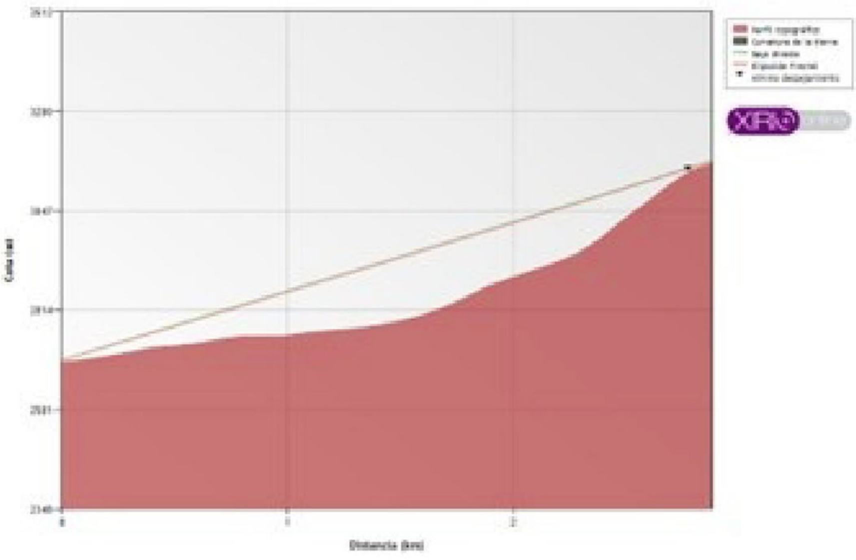

Figure 8. Path profile for Link A.
Note. Author's own elaboration based on data from Xirio Online [6].

The quantitative parameters extracted from the digital link report are consolidated in Table 8. A notable technical highlight is the fade margin of 23.95 dB, which provides a substantial safety buffer against environmental attenuation. Furthermore, the calculated annual availability reached 99.9998%, corresponding to a cumulative annual downtime of approximately one minute. This level of reliability exceeds standard requirements for rural telecommunications infrastructure.

Table 8. Simulation Parameter Summary for Link A.

Parameter	Obtained Value
Minimum Clearance	8.61 m (386.46 %)
Diffraction Attenuation	0 dB
Received Signal Level (RSL)	-63.05 dBm
Fade Margin	23.95 dB
Design Rainfall Intensity	25 mm/h
Annual Availability	99.9998% (1 min/year)

Note. Data extracted from the link report generated by Xirio Online [6].

Additionally, a point-to-point signal level report was generated to characterize propagation behavior across the entire trajectory. These discrete values, which track signal strength from the source to the destination, are presented in Table 9. This granular analysis allows the identification of any significant power drops caused by specific terrain features before the signal reaches the relay node.

Table 9. Signal Levels Along the Path for Section A.

Distance (km)	Elevation (m)	Signal Level - Direct Path (dBm)
0	2691.91	---
0.099	2697.65	-21.35
0.199	2705.51	-27.08
0.298	2715.26	-30.21
0.397	2725.57	-32.41
0.497	2729.67	-34.76
0.596	2735.31	-37.13
0.696	2745.19	-37.66
0.795	2751.89	-38.87
0.894	2752.02	-56.99
0.994	2753.41	-69.75

(continúa)

(viene)

Distance (km)	Elevation (m)	Signal Level - Direct Path (dBm)
1.093	2760.56	-67.66
1.192	2765.61	-69.04
1.292	2769.82	-71.01
1.391	2776.86	-70.18
1.491	2786.52	-65.51
1.59	2800.27	-53.02
1.689	2818.65	-45.44
1.789	2842.72	-45.49
1.888	2869.73	-45.53
1.987	2888.17	-45.79
2.087	2906.65	-46.06
2.186	2923.94	-46.34
2.286	2946.36	-46.53
2.385	2980.65	-46.56
2.484	3024.62	-46.51
2.584	3062.37	-46.57
2.683	3103.63	-46.62
2.782	3138.47	-46.75
2.882	3157.14	-47.03

Note. Author's own elaboration based on data from Xirio Online [6].

2.2. Simulation Results for Section B (Hill → School)

The second link, spanning a distance of 8.1 km, was subjected to the same analytical rigor to evaluate its performance over a significantly longer trajectory. Figure 9 illustrates the topographic path profile, evidencing that despite the increased distance, Fresnel zone clearance is maintained. This verification is essential, as it confirms that Earth curvature and intermediate orographic elevations do not interfere with the primary signal propagation volume, thereby avoiding significant diffraction-related attenuation.

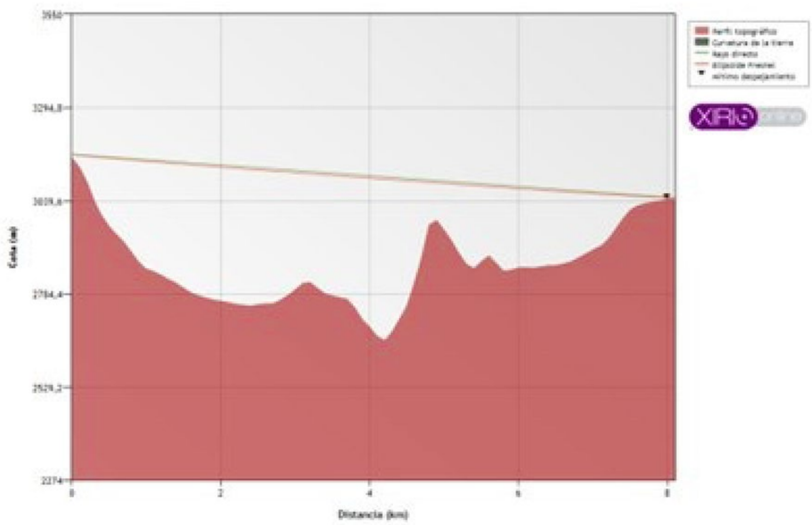

Figure 9. Path profile for Section B.
Note. Author's own elaboration based on data from Xirio Online [6].

The quantitative results derived from the digital link report for this second section are consolidated in Table 10. Despite the inherent increase in Free Space Path Loss (FSPL) due to the 8.1 km span, the system maintains robust operational indicators, validating the strategic selection of high-gain antennas and optimized transmission power levels discussed previously.

Table 10. Simulation Parameter Summary for Section B.

Parameter	Obtained Value
Minimum Clearance	5.43 m (240.03 %)
Diffraction Attenuation	0 dB
Received Signal Level (RSL)	-62.96 dBm
Fade Margin	22.04 dB
Design Rainfall Intensity	25 mm/h
Annual Availability	99.9998% (1 min/year)

Note. Data extracted from the digital link report generated by Xirio Online [6].

Furthermore, Table 11 details the signal levels calculated by the simulator at discrete intervals along the path. This spatial analysis of received power provides a deterministic view of signal degradation over distance and confirms that the final Received Signal Level (RSL) at the destination node remains within the high-modulation threshold required to meet the project's bandwidth objectives.

Table 11. Signal Levels Along the Path for Section B.

Distance (km)	Elevation (m)	Signal Level - Direct Path (dBm)
0	3157.14	---
0.2	3092.22	-36.66
0.4	2999.15	-86.15
0.6	2947	-55.5
0.8	2898.46	-46.53
1	2852.75	-47.28
1.1	2845.07	-47.08
1.3	2824.05	-47.39
1.5	2800.45	-47.98
1.7	2779.86	-48.55
1.9	2767.65	-49.01
2.1	2760.12	-49.44
2.3	2753.22	-49.88
2.499	2754.77	-50.25
2.699	2757.28	-50.62
2.899	2779.97	-50.85
3.099	2813.26	-51.03
3.299	2799.2	-51.53
3.499	2778.5	-52.03
3.699	2769.06	-52.45
3.899	2713.5	-60.8
4.099	2667.96	-62.74
4.299	2680.32	-79.92
4.499	2750.82	-53.52
4.699	2884.94	-52.56
4.899	2984.61	-52.15
5.099	2928.24	-71.4
5.299	2864.48	-74.89
5.499	2872.67	-75.9
5.699	2867.83	-80.95
5.899	2849.15	-83.97
6.099	2855.97	-81.44
6.299	2858.38	-79.02
6.499	2861.75	-86.6
6.699	2872.21	-82.53
6.899	2893.7	-71.1
7.099	2915.43	-55.34
7.298	2961.74	-55.36

(continúa)

(viene)

Distance (km)	Elevation (m)	Signal Level - Direct Path (dBm)
7.498	3014.81	-55.36
7.698	3032.16	-55.52
7.898	3039.2	-55.7
8.098	3042.28	-55.9

Note. Author's own elaboration based on data from Xirio Online [6].

2.3. Comparative Analysis of Theoretical and Simulated Results

To conclude the performance evaluation, a cross-validation was conducted between the initial mathematical models and the deterministic results obtained via simulation software. Table 12 provides a direct comparison of the key link budget parameters, contrasting the primary power metrics derived from manual theoretical calculations with the high-fidelity outputs generated by the simulation platform. This comparison is essential to quantify the impact of real-world variables such as high-resolution topographic data and standardized ITU propagation models on idealized free-space estimates.

Table 12. Power Budget Comparison: Theoretical Calculation vs. Simulation.

Parameter	Section A (Theoretical)	Section A (Simulation)	Section B (Theoretical)	Section B (Simulation)
Received Signal Level (RSL)	-64.22 dBm	-63.05 dBm	-64.53 dBm	-62.96 dBm
Fade Margin	20.78 dB	23.95 dB	20.47 dB	22.04 dB

Note. The reference receiver sensitivity Rs is -85 dBm for the theoretical calculation and -87 dBm according to the simulation report. Data extracted from Xirio Online simulation [6].

3. DISCUSSION AND CONCLUSIONS

The analysis derived from the professional simulation confirms the robustness and technical viability of the design. The data corroborates that the applied methodology, based on theoretical calculations and power optimization, is effective and achieves a solution that meets and even exceeds the requirements for high-availability networks.

3.1. Link Budget and Availability Analysis

The reliability of the design is demonstrated in the final power budget. As presented in Table 12, the clear-sky fade margins were 23.95 dB for Section A and 22.04 dB for Section B. These values exceed the minimum recommended threshold of 20 dB and ensure that the connection can withstand adverse weather conditions, such as rainfall of up to 25 mm/h, without affecting service continuity.

Similarly, the Received Signal Level (RSL) values of -63.05 dBm and -62.96 dBm fall within the ideal range defined by the -65 dBm target. This validates the adopted optimization strategy and allows the equipment to operate with high efficiency and stability, achieving an availability of 99.998% on both links.

3.2. Propagation Behavior and Fresnel Clearance

A key advantage of the simulation was the ability to represent real propagation phenomena, such as multipath fading. Although the topographic profiles show Fresnel zone clearances of 386% and 240%, respectively—values well above the 100% required to guarantee an unobstructed path—the terrain profile generates natural reflections that affect the signal.

The software facilitated the identification of these variations. In Section A, the minimum recorded power was -71.01 dBm, a value 16 dB above the receiver sensitivity of -87 dBm, which confirms that the link maintains a wide safety margin. In Section B, greater variability was observed due to valley topography, with a maximum attenuation of -86.6 dBm in an intermediate zone. However, this drop is inherent to the path and does not compromise overall stability, as the 22.04 dB fade margin acts as an energy reserve to absorb these localized losses and ensure reliable communication.

3.3. Innovation in the Autonomous Energy System

One of the innovative aspects of the project is the energy system architecture, which supplies the entire system through direct current (DC). This configuration addresses the power requirements of the Cerro La Pita node, which lacks conventional electrical infrastructure. The advantage of avoiding the use of inverters and AC/DC transformers lies in the reduction of conversion losses and the simplification of maintenance, which is essential for an autonomous system. This efficiency optimizes the use of solar energy and reduces potential points of failure, allowing the relay node to operate continuously and reliably without dependence on the commercial power grid.

3.4. Social Impact and Conclusions

This proposal enables the implementation of smart agriculture services and educational programs for the rural school, contributing to bridging the digital divide in the Buenos Aires district. Since the 5.8 GHz band is unlicensed, it is recommended to conduct an on-site spectrum analysis during installation to identify the cleanest channels and optimize system performance.

Finally, a complete and validated technical design for a high-availability radio link network in a rural environment has been achieved. The system is technically robust, with wide fade margins and reliable performance under the climatic and geographic conditions of the region. This work defines an economically replicable model for the technological development of rural communities in Colombia, demonstrating that the integration of theoretical design and professional simulation constitutes a valid, reliable, and practical solution for end users.

REFERENCES

[1] L. Suárez, "Internet rural en Colombia: Precios, empresas y cobertura en el país," *Impacto TIC*, 2025. [Online]. Available: https://impactotic.co/innovacion/internet-en-zonas-rurales-en-colombia/

[2] The Network Installers, "¿Cuál es el costo de instalación de fibra óptica?," 2025. [Online]. Available: https://thenetworkinstallers.com/es/blog/costo-de-instalacion-de-fibra-optica/

[3] Starlink, "Residencial: Internet de alta velocidad," 2025. [Online]. Available: https://www.starlink.com/co/residential

[4] J. M. Albornoz, "Radioenlaces digitales," Universidad de Los Andes, 2007. [Online]. Available: https://www.researchgate.net/publication/44419688_Radioenlaces_Digitales_Jose_Manuel_Albornoz

[5] A. Bruno and S. Jordan, *CCDA 200-310 Official Cert Guide*, 5th ed., Cisco Press, 2016, pp. 1–614. [Online]. Available: https://www.ciscopress.com/store/ccda-200-310-official-cert-guide-9781587144547

[6] ACORDE Technologies, "Xirio Online: Software de planificación de radio," 2025. [Online]. Available: https://www.xirio-online.com/

[7] International Telecommunication Union (ITU), "Recommendation ITU-R P.530-17: Propagation data and prediction methods required for the design of terrestrial line-of-sight systems," 2017. [Online]. Available: https://www.itu.int/rec/R-REC-P.530/en

[8] Google, "Google Earth Pro, ver. 7.3.6," 2025. [Online]. Available: https://www.google.com/earth/versions/#earth-pro

[9] H. Paz Penagos, R. Ferro Escobar, and E. A. Aguirre Buenaventura, *Introducción a granjas inteligentes y generación de energía eléctrica para hacer frente al cambio climático en la región andina*, Universidad Distrital Francisco José de Caldas, 2021. [Online]. Available: https://doctoradoingenieria.udistrital.edu.co/wp-content/uploads/2023/08/5-GRANJAS-INTELIGENTES-Y-GENERACION-DE-ENERGIA-ELECTRICA-PARA-HACER-FRENTE-AL-CAMBIO-CLIMATICO.pdf

[10] Trina Solar, "Datasheet Vertex N NEG19RC.20 bifacial dual glass 625W+," 2024. [Online]. Available: https://static.trinasolar.com/sites/default/files/Datasheet_210R_NEG19RC.20_EN_2024A_web.pdf

[11] SRNE Solar, "User manual MPPT solar charge controller ML2420/ML2430/ML2440," 2020. [Online]. Available: https://www.srnesolar.com/wp-content/uploads/2020/11/MPPT-Solar-Charge-Controller-ML2420-Instructions-1.pdf

[12] PowerTech Systems, "Datasheet PowerBrick+ PRO 12V 150Ah: Lithium-ion LiFePO4 battery," 2024. [Online]. Available: https://www.powertechsystems.eu/wp-content/uploads/specs/PowerBrick_PRO+_12V_150Ah_Lithium-Ion_battery.pdf

[13] B. Hauke, "Basic calculation of a buck converter's power stage," Texas Instruments, Application Report SLVA477B, 2015. [Online]. Available: https://www.ti.com/lit/an/slva477b/slva477b.pdf

[14] RADWIN, "Technical specifications RW-7401-6006 IDU-H managed indoor unit," 2024. [Online]. Available: https://www.winncom.com/pdf/Radwin_RW_7401_6006/RW-7401-6006.pdf

[15] Agencia Nacional del Espectro (ANE), "Resolución No. 000105: Por la cual se atribuyen unas bandas de frecuencias de uso libre," 2020. [Online]. Available: https://www.ane.gov.co/Documentos%20compartidos/ArchivosDescargables/noticias/RESOLUCI%C3%93N%20No%20000105%20DE%2027-03-2020(1).pdf

[16] J. L. Carrillo and J. C. Monge, "Diseño de una red digital para el Instituto Geofísico de la Escuela Politécnica Nacional," Escuela Politécnica Nacional, 2008. [Online]. Available: https://bibdigital.epn.edu.ec/bitstream/15000/910/1/CD-1799%282008-11-19-10-53-10%29.pdf

[17] UNESCO, “Educación para las poblaciones rurales: Aplicación de las TIC para el acceso a una educación de calidad para la población rural; informe final,” 2004. [Online]. Available: https://unesdoc.unesco.org/ark:/48223/pf0000159966

[18] ISTE, “Standards for students: Empowering learners through interactive technology,” 2024. [Online]. Available: https://www.iste.org/standards/iste-standards-for-students

[19] Ministerio de Educación Nacional, “Plataforma Colombia Aprende: Recursos educativos digitales para la ruralidad,” 2024. [Online]. Available: https://www.colombiaaprende.edu.co/

[20] Ministerio de Tecnologías de la Información y las Comunicaciones (MinTIC), “Programa de formación y capacitación docente en apropiación de TIC,” 2023. [Online]. Available: https://www.mintic.gov.co/portal/715/w3-article-150613.html

[21] Google Support, “Velocidad de conexión y requisitos del sistema para ver videos en YouTube,” 2024. [Online]. Available: https://support.google.com/youtube/answer/78358

[22] Federal Communications Commission (FCC), “Broadband speed guide,” 2022. [Online]. Available: https://www.fcc.gov/consumers/guides/broadband-speed-guide